First results of the ARGO-YBJ experiment operated in Scaler Mode

Piero Vallania*, Tristano Di Girolamo† and Carlo Vigorito‡ for the ARGO-YBJ Collaboration
*INAF-IFSI Torino and INFN, Sezione di Torino, Via P. Giuria 1, 10125 Torino, Italy
†Dip. di Fisica dell'Università di Napoli and INFN, Sezione di Napoli, via Cinthia, 80126 Napoli, Italy
‡Dip. di Fisica Generale dell'Università di Torino and INFN, Sezione di Torino, Via P. Giuria 1, 10125 Torino, Italy
Email: Piero.Vallania@to.infn.it, Carlo.Vigorito@to.infn.it, Tristano.DiGirolamo@na.infn.it

***Abstract*— The aim of the ARGO-YBJ Extensive Air Shower experiment is to operate in the field of High Energy Cosmic Ray Physics with an energy threshold of a few hundreds of GeV, performing a detailed imaging of the shower disk. This is obtained with both a high altitude location (in Tibet, P.R. China, at 4300 m a.s.l.) and a large area full coverage (6700 m^2) and high granularity detector. The experiment is working in both "shower mode" and "scaler mode", the latter consisting in recording the detector counting rates from singles to four-fold coincidences in a fixed time window of 500 ms. This technique does not allow the measurement of the arrival direction of each primary, due to the limited number of particles per shower, but gives the possibility to reach the lowest energy limit of the detector (E $>$ 1 GeV) and to study the temporal behaviour of the high energy emission of transient phenomena in coincidence with satellite or ground measurements, mostly operating at lower energies. A large fraction of the detector is in data taking and the first results on the search for GRBs are presented.**

I. Introduction

The study of the energy region between 1 and 100 GeV is difficult from both space and ground level for different reasons. In space it is hampered by the very low fluxes, requiring a large collection area; at ground level the small number of secondary particles increases the energy threshold of air shower arrays (at sea level we expect $2.9{\cdot}10^{-6}$ particles/gamma shower at 1 GeV and $5.2{\cdot}10^{-2}$ at 100 GeV) and requires huge Imaging Atmospheric Cherenkov Telescopes (IACTs). Nevertheless the EGRET instrument on board CGRO had a 20 GeV high energy limit; currently, waiting for GLAST, no satellite detector is working in this energy range. On the other hand, with the second generation of IACTs the energy threshold has been pushed as low as 30 GeV [1]. In this energy region, apart from steady gamma ray sources, transient phenomena are expected, the most intriguing being Gamma Ray Bursts (GRBs). Three of them have been detected by EGRET with $E_{max} > 1$ GeV, and a maximum photon energy of 18 GeV [2]. This proves that the 1-100 GeV energy region is surely covered by this phenomenon; the extension of the GRB emission to higher energies could provide extremely useful information to constrain theoretical models. In the same energy range, other interesting phenomena, much closer to us, are gamma rays from solar flares and high energy proton emissions from the Sun causing short increases of the ground detector counting rate (Ground Level Enhancements).

Ground experiments usually detect air showers through the coincidence of different detector units. This "shower mode" technique can be joined by the "scaler mode", counting the number of events in a fixed time window. Since the small number of detected secondary particles per shower (often just one) does not allow the measurement of the primary particle arrival direction, this technique needs a trigger by a different experiment to detect a transient emission of charged or gamma ray primaries as a statistically significant and coincident excess of events over the uniform background due to cosmic rays. In order to obtain the best benefit from this technique, a huge detector located at high altitude is required. The ARGO-YBJ experiment, with its detection area of $\sim$ 6700 m^2 at an altitude of 4300 m a.s.l., where $3.5{\cdot}10^{-3}$ particles are expected at 1 GeV and 13.8 at 100 GeV, is the most sensitive among present and past detectors.

II. The detector

The ARGO-YBJ experiment is located at the YangBaJing Cosmic Ray Laboratory (longitude 90.53°E, latitude 30.11°N). Made by a single layer of Resistive Plate Chambers (RPCs), it has a modular structure, the basic module being the "cluster" (5.7 x 7.6 m^2), divided into 12 RPCs (2.8 x 1.25 m^2 each). 130 of these clusters, constituting the complete full coverage central carpet, with $\sim$ 93% of active area, are in operation since August 2006; the installation of 24 additional clusters surrounding the central detector ("guard ring"), with a coverage of $\sim$ 40%, has been completed in October 2006 and they will be included in the data acquisition within the end of 2006. Each RPC is read by 80 "strips" of 6.75 x 61.8 cm ^{2}, logically organized in 10 "pads" of dimension 55.6 x 61.8 cm^2, which represent the high granularity pixels of the detector. For the "scaler mode" technique, the counts from different pads of the same cluster are put in coincidence in a narrow time window (150 ns), producing higher multiplicities. For each cluster, four different channels, corresponding to multiplicities $\geq$1, $\geq$2, $\geq$3 and $\geq$4, are acquired by 4 different scalers every 500 ms, with measured rates of 40 kHz, 2 kHz, 300 Hz and 120 Hz, respectively.

III. Counting rate stability and expected statistical distribution

As explained in the previous section, the counting rates from each cluster are acquired indipendently. Since the significance

of a detection or the upper limits to a signal are connected to the real counting rate distribution, the knowledge of the detector behaviour is crucial to correctly evaluate the excess significance. For this reason we have studied the counting rate distribution for fixed multiplicities, i.e. for $C_i = C_{\geq i} - C_{\geq i+1}$, i=1,3. Figure 1 shows these distributions for a typical cluster, together with the total counting rate obtained adding up the 4 multiplicity channels. They include 30 minutes of continuous

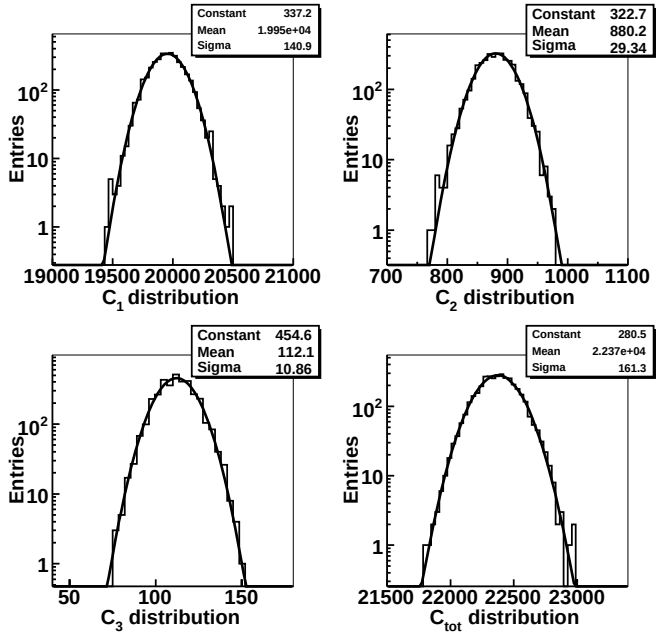

Fig. 1. Counting rate distributions for a typical cluster.

data acquisition; for longer durations, the effects due both to environmental parameters, such as the atmospheric temperature and pressure (which modify the shower development in the atmosphere), and to instrumental parameters, such as the experiment building temperature (which modify the detector efficiency), start to be relevant (see Figure 2). Another peculiarity of the RPC detectors is their sudden discharge when hit by a high density shower, causing the narrow downgoing peaks evident in Figure 2. These discharges, followed by an exponential recharge with a typical time constant of a few tens of seconds, must be carefully identified and taken into account.

Figure 1 shows that each multiplicity follows a Poisson distribution while their sum, due to the correlation between the different channels given by the shower itself, follows a larger distribution with a σ^2 given by:

$$\sigma^2(C_{tot}) = \sigma^2(C_1) + 4\cdot\sigma^2(C_2) + 9\cdot\sigma^2(C_3) + 16\cdot\sigma^2(C_4) \quad (1)$$

where C_i are the counts for a given multiplicity for each cluster, $\sigma^2(C_i)$ is the Poissonian width of each distribution and $\sigma^2(C_{tot})$ is the resulting width of the total multiplicity: $C_{tot} = C_1 + 2\cdot C_2 + 3\cdot C_3 + 4\cdot C_4$.

For our purposes, the maximum sensitivity of the detector is obtained adding up all the multiplicities of the clusters; however, since each multiplicity corresponds to a different

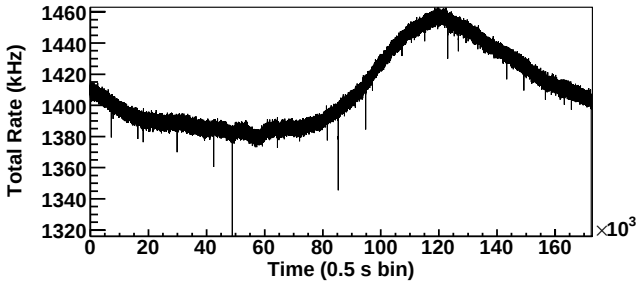

Fig. 2. Counting rate of the whole ARGO-YBJ detector as a function of time during a period of 24 hours.

energy region, we also separate the multiplicities in order to study the energy region of interest in different bins. In both cases we have to study the statistical behaviour of these sums. Adding up the same counting channel for different clusters, we must consider the probability that one single event can satisfy the same trigger condition on different clusters generating correlated counts which enlarge the expected Poissonian distribution. The analytical calculation gave the following result: for

$$N_{tot} = \sum_{i=1}^{n} N_i, \quad \sigma^2_{N_{tot}} = < N_{tot} > (1 + \sum_{i=2}^{n} (i^2 - i)\cdot p_i) \quad (2)$$

where N_i is the number of events for which the trigger condition is satisfied only on i detectors and $p_i = N_i/N_{tot}$ are the corresponding probabilities. The width of this distribution is larger than the expected Poissonian value $\sigma^2_{N_{tot}} = < N_{tot} >$. Since the p_i values depend on the trigger, the lateral distribution function and the detector configuration, they must be evaluated using a MonteCarlo (MC) simulation. This simulation, now in progress, will be used to verify that the width of the distribution of the integral counting rates corresponds to what expected from the correlation of particles inside the showers. Actually this effect can be measured by the experimental data provided that the distributions for each cluster and channel are Poissonian.

IV. GRB SEARCH: THE METHOD

In order to search for a GRB and correctly evaluate the significance of a possible signal, the following method has been implemented.

1. For each cluster and each multiplicity, a period of ± 12 hours around the GRB time has been analized to check the detector perfomance. Let's consider a reference *signal* s of duration 10 s, and a reference *background* b of duration 100 s both before and after the signal: s and b are integrated over the corresponding durations. Then we define the normalized fluctuation

$$f = (s - b)/\sigma, \quad \sigma = \sqrt{b + b/20} \quad (3)$$

which represents the significance of the signal to the background fluctuation. Over 24 hours of data a total of $86400/210 \approx 411$ trials are performed and the distribution of f values is obtained for each counting channel. The upper plot of Figure 3 shows the result for a good channel compared

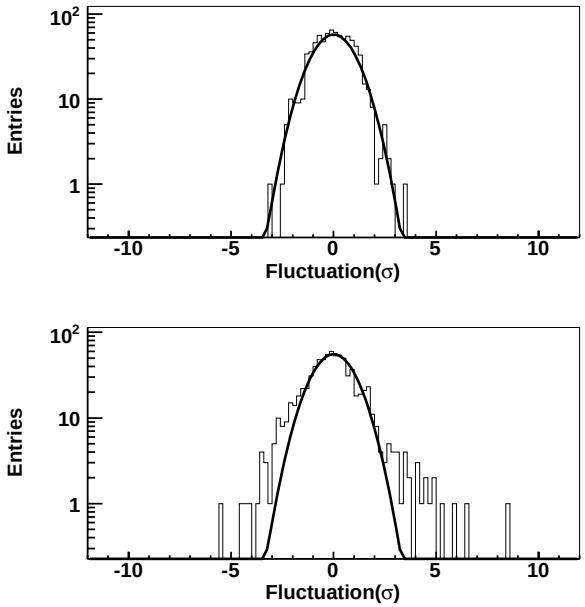

Fig. 3. Distribution of normalized excesses of signal to background compared with the expected normalized Gaussian distribution. Top: good counting channel; bottom: bad counting channel, showing non-Poissonian fluctuations.

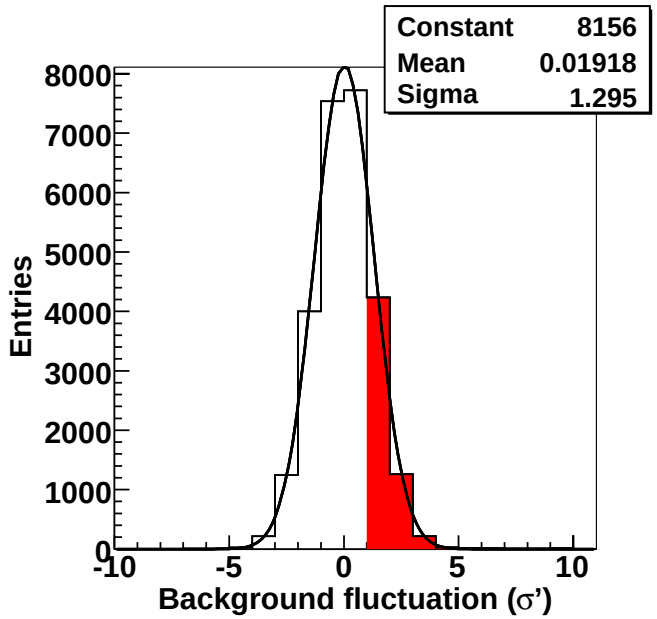

Fig. 4. Distribution of normalized excesses of signal to background for GRB060717, fitted with a Gaussian function $G(0,\sigma')$. The plot refers to the sum of 123 clusters (C_1 counting channel).

with the expected normalized Gaussian distribution while the lower one shows a channel having anomalous non-Poissonian fluctuations. Studying the behaviour of f we can classify good and bad channels at the GRB time, discarding the second ones in the refined analysis of the GRB event. Note that, even if the counting rate is Poissonian only for periods $\lesssim$ 1 hour, the fluctuations f are Poissonian for a longer period, due to the short reference duration adopted for both signal and background. The long term variations, as shown in Figure 2, can thus be neglected and the single channel response always results "locally" Poissonian.

2. The technique is now exploited for the analysis of each GRB: the signal s has a duration T90 and the background b $10 \times T90$ before and after the burst time T0. In order to maximize the sensitivity, the integration of the counting rates of all good clusters is performed: only C_1 channels are considered to have the lowest energy threshold. The experimental distribution of f is obtained over $86400/T90$ trials: the distribution, as pointed out in the previous section, is no longer a Poissonian but a Gaussian G(0, $\sigma^{'}$) with $\sigma^{'} > 1$ which accounts for the correlation effects. Figure 4 shows the distribution of f observed for GRB060717: the red dashed area indicates the fraction of background events above the significance of the GRB signal (see Table I). This plot describes correctly the background behaviour at the time of the event. Therefore the significance associated to the GRB, i.e., the significance normalized to the spread of the f distribution, is:

$$n_\sigma = \frac{(s_{GRB} - b_{GRB})/\sqrt{b_{GRB} + b_{GRB}/20}}{\sigma^{'}} \qquad (4)$$

where s_{GRB} is the signal starting at T0 with duration T90, and b_{GRB} is the background measured before and after the event for a total duration of $20 \times T90$. In case of no detection, the upper limit on the GRB fluence is obtained from relation (4) using the value of s_{GRB} corresponding to n_σ = 3.

V. Effective Areas and Convolution with Primary Spectra

The sensitivity of the ARGO-YBJ experiment in detecting small Extensive Air Showers produced by both protons and photons has been studied by a detailed MC simulation based on the CORSIKA/QGSjet code 6.204 [3]. Events with fixed energies in the range 1 GeV-1 TeV and fixed zenith angles θ = $0°, 10°, 20°, 30°$,$40°$ have been generated, with a full development of the electromagnetic component down to E_{th}=0.05 MeV for both electrons and photons, and 50 MeV for muons and hadrons. Since we are interested also to single particles, a huge sampling area is needed to fully contain the lateral distribution even at these energies; in order to save computing time, the "reciprocity method" [4] has been used, allowing us to choose a sampling area of 5000 x 5000 m^2. The detector has been simulated in a simplified way, since the only important effect that we must take into account is the *"strip multiplicity"*, i.e., the relation between the number of particles hitting the detector and the measured multiplicity, due to the detector efficiency and the strip cross talk [5]. Figure 5 shows the effective areas for primary photons and protons with zenith angle θ=$20°$ in four different multiplicity channels. Folding these effective areas with the following spectra: $dN_\gamma/dE \propto E^{-2}$ up to E_{max} = 100 GeV for photons, and $dN_p/dE \propto E^{-2.7}$ for protons [6] (taking into account the local geomagnetic cutoff [7]), we obtain the mean primary energy values listed in Table II. The spectral index adopted for photons corresponds to the mean value for GRBs as measured by EGRET [8].

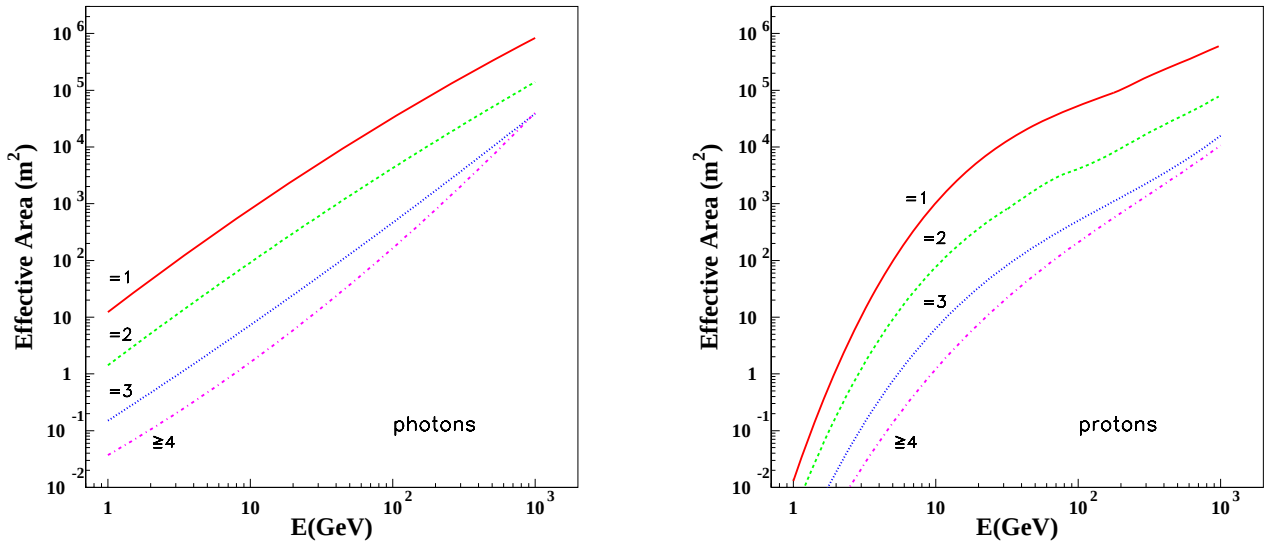

Fig. 5. Effective areas as a function of primary energy for photons (left) and protons (right). The curves refer to multiplicities C_1, C_2, C_3, $C_{\geq 4}$ and zenith angle θ = 20°.

TABLE I

LIST OF GRBS WITH ZENITH ANGLE $\theta \leq 40°$ (DECEMBER 2004 - MAY 2006), WITH CORRESPONDING 3σ FLUENCE UPPER LIMITS.

GRB	Sat.	T90/Dur. (s)	θ^* (deg)	Redshift	Spectral Index	Carpet Area (m^2)	$n_\sigma^\S$	UL† (Fluence)
041228	Swift	62	28.1	–	1.56	693	-0.34	$5.8{\cdot}10^{-4}$
050408	HETE	15	20.4	1.24	1.98	1820	-1.2	$\mathbf{1.1{\cdot}10^{-4}}$
050509A	Swift	12	34.0	–	2.1	1820	0.44	$1.8{\cdot}10^{-4}$
050528	Swift	11	37.8	–	2.3	1820	-0.03	$6.2{\cdot}10^{-4}$
050802	Swift	13	22.5	1.71	1.55	1820	0.82	$\mathbf{8.5{\cdot}10^{-5}}$
051105A	Swift	0.03	28.5	–	1.33	3379	-1.5	$1.3{\cdot}10^{-5}$
051114	Swift	2	32.8	–	1.22	3379	1.2	$2.5{\cdot}10^{-5}$
051227	Swift	8	22.8	–	1.31	3379	-0.89	$2.1{\cdot}10^{-5}$
060105	Swift	55	16.3	–	1.11	3379	1.3	$1.6{\cdot}10^{-4}$
060111A	Swift	13	10.8	–	1.63	3379	-0.54	$3.4{\cdot}10^{-5}$
060115	Swift	142	16.6	3.53	1.76	4505	0.17	$\mathbf{1.2{\cdot}10^{-3}}$
060421	Swift	11	39.3	–	1.53	4505	-0.71	$1.9{\cdot}10^{-4}$
060424	Swift	37	6.7	–	1.72	4505	-0.05	$7.6{\cdot}10^{-5}$
060427	Swift	64	32.6	–	1.87	4505	-0.39	$4.1{\cdot}10^{-4}$
060510A	Swift	21	37.4	–	1.55	4505	2.0	$3.4{\cdot}10^{-4}$
060526	Swift	14	31.7	3.21	1.66	4505	0.63	$\mathbf{1.5{\cdot}10^{-4}}$
060717	Swift	3	7.4	–	1.72	5632	1.08	$1.3{\cdot}10^{-5}$
060801	Swift	0.5	16.8	–	0.47	5632	0.10	$4.8{\cdot}10^{-6}$
060807	Swift	34	12.4	–	1.57	5632	0.61	$7.6{\cdot}10^{-5}$

$*$ Zenith angle.
§ Significance of the signal for the single event.
† Upper Limits on the fluence (1 – 100 GeV) in erg cm^{-2}. The numbers in bold take into account absorption by the EBL.

Of course, the values found for photons strongly depend on the maximum energy E_{max} (never measured) and on the spectral index (measured by satellites at lower energies).

VI. RESULTS

The search for emission from GRBs started with the first GRB detection by the Swift satellite on December 17th, 2004, when only 16 clusters ($\sim$ 1/10 of the total surface) were in data taking. Due to atmospheric absorption, we selected events with zenith angle $\theta \leq 40°$. Table I reports the list of GRBs up to August 2006. The statistical significance of the signal has been calculated as explained in section IV; this represents an improvement with respect to the previously reported results, obtained with Poissonian fluctuations [9], [10]. No convincing excess has been found so far in coincidence with the T90 satellite detection; 3 σ fluence upper limits where therefore calculated for multiplicity $C = 1$ in the 1-100 GeV energy range using the spectral indices measured by satellites. When the redshift is known, a model for the Extragalactic Background Light (EBL) absorption has been adopted [11] and the corresponding fluence upper limits are printed in bold; otherwise z=0 (no absorption) was assumed. We point out that the fluence upper limits depend on the energy range, spectral index and maximum energy considered; however, with the above assumptions, they are the lowest limits obtained in this energy range by all present and past ground based detectors. Figure 6 shows the distribution of the statistical significances of the analyzed GRBs, compared with a normalized Gaussian

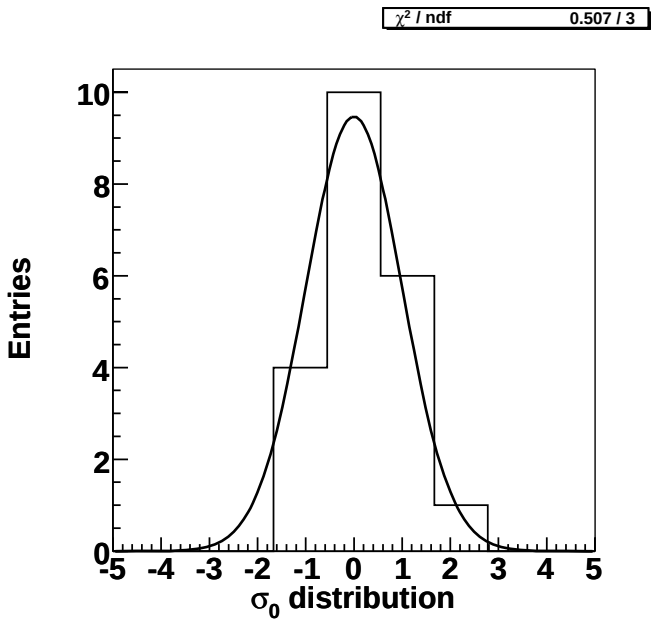

Fig. 6. Distribution of the statistical significances of the 19 GRBs listed in Table I, compared with a normalized Gaussian function.

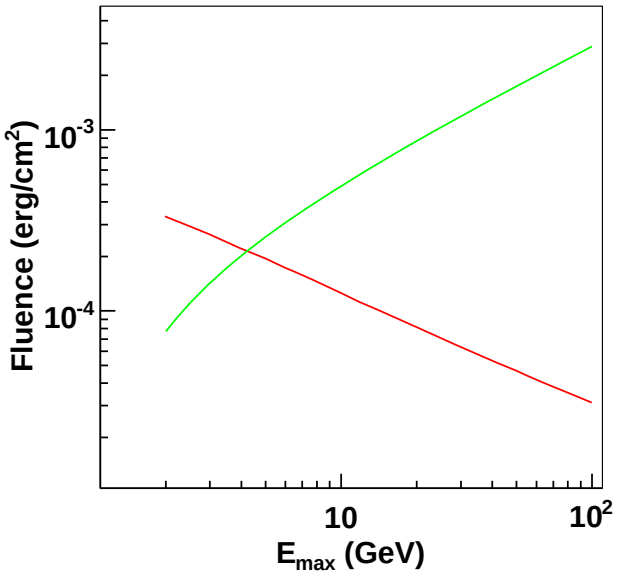

Fig. 7. Fluence extrapolation of GRB051227 (dotted line) compared with our 3σ upper limit (full line) as a function of the cutoff energy E_{max}. The two lines cross at a value corresponding to our upper limit to $E_{max} \sim 4\ GeV$.

TABLE II

MEAN PRIMARY ENERGIES FOR PHOTONS AND PROTONS

Cluster Multiplicity	$\bar{E}_\gamma$ (GeV)	$\bar{E}_p$ (GeV)
n = 1	41	104
n = 2	43	138
n = 3	45	172
n $\geq$ 4	50	248

function. Even if the statistics is very poor, the two distributions are consistent, proving that we are observing background signals and that the significances are correctly evaluated.
Finally, we have compared the extrapolation of the spectrum of GRB051227, which has one of the flattest measured spectra, with our upper limits, obtained for a cutoff energy E_{max} ranging from 2 to 100 GeV. Figure 7 shows the result of this comparison: the dotted line represents the extrapolated fluence as a function of E_{max}, while the full line is our 3σ upper limit. The two lines cross at $\sim$4 GeV, corresponding to our upper limit to the maximum energy for this GRB. Even if the spectral index is measured at a very lower energy (15-150 keV), and a bend at an intermediate energy is expected [12], we see that for this GRB a spectrum extending over 4 GeV is excluded by our limit.

VII. CONCLUSION

An accurate study of the statistical behaviour of the ARGO-YBJ detector has been carried out in order to correctly evaluate the statistical significance of excesses in the counting rate. For short-term variations ($\lesssim$ minutes), the detector behaves Poissonian for each cluster and multiplicity, the non-Poissonian behaviour of the counting rate being due to the correlation between different clusters given by the shower lateral distribution. The distribution of the significance of the excesses for 19 GRBs exploded within a zenith angle $\theta \leq 40^\circ$ in the period December 2004 - August 2006 is consistent with a background distribution, showing that no significant excess has been found. Nevertheless, a constrain to the maximum energy can be already set at least for the strongest GRBs, as shown for GRB051227. These results were obtained during the ARGO-YBJ installation, with an area increasing from 1/10 to the almost complete detector. Now the full central carpet is in data acquisition and the guard ring will be installed before the end of 2006. Moreover, a 0.5 cm thick layer of lead ($\sim$ 1 radiation length) will be put over the RPCs to convert secondary photons, with an expected increase in the sensitivity of a factor $\sim$ 2. In conclusion ARGO-YBJ, the most sensitive experiment for the detection of the high energy tail of GRB spectra, is almost ready to work at its best performance.

REFERENCES

[1] D. Bastieri et al., "The MAGIC Experiment and Its First Results", Proc. 6th International Symposium "Frontiers of Fundamental and Computational Physics" (Udine, Italy, 2004), in press, astro-ph/0503534.
[2] J.R. Catelli et al., in *"Gamma Ray Bursts"*, edited by C.A. Meegan, AIP Conf. Proc. No. 428, p.309 (AIP, New York, 1998).
[3] Heck, D. et al., Report FZKA 6019 Forshungszentrum Karlsruhe, 1998.
[4] G. Battistoni et al., Astrop. Physics 7 (1997) 101.
[5] X. Sheng et al., Proc. 29th ICRC (2005), Vol.5, p.151.
[6] T.K. Gaisser and M. Honda, *Ann. Rev. Nucl. Part. Sci. 52* (2002) 153.
[7] M. Storini, D.F. Smart and M.A. Shea, 27th ICRC (2001), Vol.10, p.4106.
[8] B.L. Dingus, J.R. Catelli and E.J. Schneid, 25th ICRC (1997), Vol.3, p.30.
[9] G. Di Sciascio and T. Di Girolamo for the ARGO-YBJ Collaboration, Proc. of the Workshop "The Multi-Messenger Approach to High Energy Gamma Ray Sources" (Barcelona, Spain, July 2006), in press, astro-ph/0609317.
[10] I. James for the ARGO-YBJ Collaboration, Proc. of the Workshop "Science with the New Generation of High Energy Gamma Ray Experiment" (Isola d'Elba, Italy, June 2006), in press.
[11] T.M. Kneiske et al., *A&A* 413 (2004) 807.
[12] R.D. Preece et al., *ApJS* 126 (2000) 19.